Structural Engineering and Mechanics, *Vol. 75, No. 6 (2020) 771-784*
DOI: https://doi.org/10.12989/sem.2020.75.6.771

A novel reliability analysis method based on Gaussian process classification for structures with discontinuous response

Yibo Zhang*, Zhili Sun, Yutao Yan, Zhenliang Yu and Jian Wang

School of Mechanical Engineering and Automation, Northeastern University, Wenhua Road, Heping District, Shenyang 110819, Liaoning, People's Republic of China

(Received October 18, 2019, Revised April 30, 2020, Accepted May 1, 2020)

Abstract. Reliability analysis techniques combining with various surrogate models have attracted increasing attention because of their accuracy and great efficiency. However, they primarily focus on the structures with continuous response, while very rare researches on the reliability analysis for structures with discontinuous response are carried out. Furthermore, existing adaptive reliability analysis methods based on importance sampling (IS) still have some intractable defects when dealing with small failure probability, and there is no related research on reliability analysis for structures involving discontinuous response and small failure probability. Therefore, this paper proposes a novel reliability analysis method called AGPC-IS for such structures, which combines adaptive Gaussian process classification (GPC) and adaptive-kernel-density-estimation-based IS. In AGPC-IS, an efficient adaptive strategy for design of experiments (DoE), taking into consideration the classification uncertainty, the sampling uniformity and the regional classification accuracy improvement, is developed with the purpose of improving the accuracy of Gaussian process classifier. The adaptive kernel density estimation is introduced for constructing the quasi-optimal density function of IS. In addition, a novel and more precise stopping criterion is also developed from the perspective of the stability of failure probability estimation. The efficiency, superiority and practicability of AGPC-IS are verified by three examples.

Keywords: reliability analysis; discontinuous response; Gaussian process classification; small failure probability; importance sampling

1. Introduction

Reliability analysis aims at estimating structural failure probability under the influence of uncertainties in material, external loads, geometric dimensions, etc. In reliability analysis, the failure probability P_f is expressed as

$$P_f = \int_{G(\boldsymbol{x})\le 0} f_X(\boldsymbol{x})\mathrm{d}\boldsymbol{x} \tag{1}$$

where $\boldsymbol{x}$ is a vector containing M uncertainties, i.e. $\boldsymbol{x}=[x_1,\ldots, x_M]$ and $f_X(\boldsymbol{x})$ denotes the joint probability density function (PDF) of $\boldsymbol{x}$. $G(\boldsymbol{x})$ denotes the structural performance function and as long as $G(\boldsymbol{x})$ is greater than 0, the structure is safe, otherwise it fails (Jagan *et al.* 2019).

To perform the reliability analysis, various algorithms have been proposed over the last decades. They mainly include the sampling-based techniques (i.e. Monte Carlo Simulation (MCS), Line Sampling (LS) (Shayanfar *et al.* 2017), Subset Simulation (SS) (Au and Beck 2001, Zhang *et al.* 2018), Importance Sampling (IS) (Yonezawa *et al.* 2009, Yun *et al.* 2018), etc.), the approximate analytic methods (Yao *et al.* 2019) (i.e. First-order reliability method (FORM), Second-order reliability method (SORM), etc.), the numerical integration methods (i.e. Point Estimate Method (PEM) (Napa-García *et al.* 2017), Spare grid integration (SGI) (Xiong *et al.* 2010), Direct Optimized Probabilistic Calculation (DOProC) (Krejsa *et al.* 2013, 2016), etc.) and the surrogate-model-based methods (Gaspar *et al.* 2014, Zhao *et al.* 2017, Sun *et al.* 2017). When using these methods to perform the reliability analysis, the original random vector space is usually mapped into the mutually independent standard normal space in view of some unique properties of the normal distribution. The commonly used transformation techniques include Hermit polynomials (Winterstein 1988), Rackwitz-Fiessler transformation (Roudak and Karamloo 2018), Rosenblatt transformation (Wang and Li 2017), Nataf transformation (Doh *et al*. 2020), etc.

During recent years, the reliability analysis methods based on surrogate models have drawn growing attention due to their high efficiency and versatility. Generally speaking, the surrogate models can be divided into two categories: regression-based and classification-based. The regression-based models mainly include Response Surface Method (RSM) (Su *et al.* 2015, Zhao *et al.* 2016, Fang *et al.* 2017), Kriging model (Wang *et al.* 2017, Wang and Sun 2018, Zhang *et al.* 2019), Support Vector Regression (SVR) (Fei and Bai 2013), Artificial Neural Network (ANN) (Elhewy *et al.* 2006), Polynomial Chaos Expansions (PCE) (Xu and Wang 2019), etc. The classification-based ones include Support Vector Classification (SVC) (Alibrandi *et al.* 2015), ANN, Gaussian process classification (GPC) (Nguyen *et al.* 2019, Garcia-Fernandez *et al.* 2019), etc. The difference between the two categories is that the former predicts the response of sample through regression analysis, while the latter infers the class label of sample by constructing a classifier. Furthermore, the regression-based

*Corresponding author, Ph.D. Student
E-mail: neuzyb@163.com

ISSN: 1225-4568 (Print), 1598-6217 (Online)

models only deal with the problem whose output is continuous, while the classification-based ones can handle the case where the output is continuous or discontinuous. Although various surrogate-model-based reliability evaluation algorithms have been proposed, they are primarily confined to the structures with continuous response. However, there are many structures with discontinuous response in engineering practice, i.e. arch structures, truss structures, structures involving collision and impact, etc. Unfortunately, the researches on the reliability analysis for such structures are rare and primarily based on SVC or ANN (Alibrandi *et al.* 2015). Nevertheless, those methods based on SVC or ANN still have some intractable defects. ANN requires large numbers of labeled samples and a long training time for obtaining an accurate estimation of failure probability. Besides of abundant labeled samples, SVC also has difficulties in reasonably determining its kernel function, kernel parameters and loss function.

GPC, as a branch of Gaussian process, has a strict theoretical basis of statistics and gains attention increasingly in machine learning. Compared with ANN and SVC, GPC has good adaptability to deal with complex problems such as small samples, high dimensionality and nonlinearity, and can adaptively obtain the optimal hyper parameters. Furthermore, GPC can also provide the predicted class label with a probabilistic significance (Garcia-Fernandez *et al.* 2019). Therefore, this paper adopts GPC to evaluate the reliability of the structures with discontinuous response.

However, the time complexity of GPC performing inference is cubic of the number of training samples (Nguyen *et al.* 2019). Moreover, the performance function should be called as little as possible when performing reliability analysis. Therefore, the adaptive DoE strategy is increasingly attracting attention and several types of GPC-based DoE strategies have been proposed from different perspectives. Kapoor *et al.* (2009) and Rodrigues *et al.* (2014) regard the sample with classification probability closest to 0.5 as the new training sample and add it to DoE. Peng *et al.* (2014) select the most probable point (MPP) as the new training sample for improving the accuracy of Gaussian process classifier and the efficiency of reliability analysis. To apply GPC to the multi-classification problems, Sun *et al.* (2015) propose three strategies to select the most valuable samples. However, the training samples selected by existing strategies are easily overlapped or clustered, which must increase redundant calls of performance function. Furthermore, when selecting the new training sample, they only consider improving the classification accuracy of the selected training sample instead of improving that of the region around it.

Moreover, MC-based adaptive DoE strategies and reliability analysis methods are no longer applicable for the structures involving small failure probability due to enormous evaluations of MC samples (Yang *et al.* 2018). Fortunately, the reliability analysis methods combining variance reduction techniques (Yun *et al*. 2017, En *et al.* 2019) (i.e. LS, SS, IS, etc.) can overcome this defect, among which IS-based methods are the most widely researched and used. Furthermore, the IS methods based on kernel density estimation (KDE) or adaptive KDE (AKDE) have advantages over those based on MPP or MPPs in efficiency and accuracy since they do not rely on MPP or MPPs and can cover the entire failure region well. Although Yang *et al.* (2018) developed a reliability evaluation technique integrating Kriging with KDE-based IS, there is no relevant research on GPC-based reliability analysis method for structures involving discontinuous response and small failure probability. Moreover, their method not only needs to utilize optimization algorithm for selecting the new training sample but employs two stages to complete the reliability evaluation, which is tedious and easily falls into the local optimum.

To this end, a creative adaptive DoE strategy, taking into account the classification uncertainty, the sampling uniformity and the regional classification accuracy improvement, is proposed in this research. Furthermore, a novel reliability analysis method combining adaptive GPC and AKDE-based IS for structures with discontinuous response and small failure probability is also developed, which is termed as AGPC-IS. This research primarily includes the following contents. Section 2 introduces the fundamental principles about GPC and IS. Section 3 introduces the AGPC-IS and its implementation procedures in detail. By several examples, Section 4 verifies its efficiency, accuracy and feasibility. Section 5 summarizes the conclusions.

2. Gaussian process classification and importance sampling

2.1 Gaussian process classification

The theoretical fundamental of GPC is compendiously introduced in this subsection. In the field of reliability, structural state is usually treated as a binary classification problem, i.e. whether it is safe or invalid. For this problem, GPC usually utilizes the class labels y=+1 or -1 to distinguish the structural state, i.e. y=+1 means that structure is safe, whereas y=-1 denotes that structure fails. According to the given N training samples $\boldsymbol{X}$ and their corresponding class labels $\boldsymbol{Y}$, GPC classifies the structural state through the mapping relationship (called latent function $f(\boldsymbol{x})$) between $\boldsymbol{X}$ and $\boldsymbol{Y}$ and simultaneously assigns a corresponding probability to the classification result (Peng *et al.* 2014).

To classify an unobserved sample $\boldsymbol{x}_*$, one must first obtain the distribution of its corresponding latent variable f_* by (Nguyen *et al.* 2019, Garcia-Fernandez *et al.* 2019)

$$p\left(f_*\middle|\boldsymbol{X},\boldsymbol{Y},\boldsymbol{x}_*\right)=\int p\left(f_*\middle|\boldsymbol{X},\boldsymbol{x}_*,\boldsymbol{f}\right)p\left(\boldsymbol{f}\middle|\boldsymbol{X},\boldsymbol{Y}\right)\mathrm{d}\boldsymbol{f} \tag{2}$$

where $\boldsymbol{f}$ denotes the vector of latent variables corresponding to $\boldsymbol{X}$, i.e. $\boldsymbol{f}=[f(\boldsymbol{x}_1), f(\boldsymbol{x}_2), \ldots, f(\boldsymbol{x}_N)]^T$, $p(f_*|\boldsymbol{X}, \boldsymbol{x}_*, \boldsymbol{f})$ represents the conditional prior distribution of latent variable f_* and $p(\boldsymbol{f}|\boldsymbol{X},\boldsymbol{Y})$ denotes the posterior distribution of latent vector $\boldsymbol{f}$.

The conditional distribution $p(f_*|\boldsymbol{X}, \boldsymbol{x}_*, \boldsymbol{f})$ relies on the joint prior distribution $p(f_*, \boldsymbol{f}|\boldsymbol{X}, \boldsymbol{x}_*)$ of f_* and $\boldsymbol{f}$. Furthermore, it is difficult to obtain the distribution $p(\boldsymbol{f}|\boldsymbol{X},\boldsymbol{Y})$. To this end, GPC first assumes that the prior distribution $p(\boldsymbol{f}|\boldsymbol{X})$ obeys

the Gaussian distribution, that is,

$$p(\boldsymbol{f}|\boldsymbol{X}) = N(\boldsymbol{m}, \boldsymbol{K}) \tag{3}$$

where $\boldsymbol{m}$ is the mean vector and $\boldsymbol{K}$ ($\boldsymbol{K}=[k(\boldsymbol{x}_i,\boldsymbol{x}_j)]_{N\times N}$) denotes the covariance matrix. In general, $\boldsymbol{m}$ is usually set to zero mean vector. Furthermore, various types of covariance functions are available, among which the Squared Exponential covariance function (SE) is the most common in use, and its expression is

$$k(\boldsymbol{x}_i, \boldsymbol{x}_j) = \sigma_f^2 \exp\left(\frac{-\|\boldsymbol{x}_i - \boldsymbol{x}_j\|^2}{2l^2}\right) \tag{4}$$

where σ_f is employed to control the extent of local correlation and the exponent part represents the distance correlation between two samples, i.e. if the distance between two samples is very small relative to the distance scale l, they are highly correlated, conversely, their correlation is low.

Subsequently, the distribution $p(f_*, \boldsymbol{f}|\boldsymbol{X}, \boldsymbol{x}_*)$ of f_* and $\boldsymbol{f}$ is

$$p(f_*, \boldsymbol{f}|\boldsymbol{X}, \boldsymbol{x}_*) = N\left(\begin{bmatrix}\boldsymbol{m}\\ m_{\boldsymbol{x}_*}\end{bmatrix}, \begin{bmatrix}\boldsymbol{K} & \boldsymbol{K}_{\boldsymbol{x}_*}\\ \boldsymbol{K}_{\boldsymbol{x}_*}^{\mathrm{T}} & k_{\boldsymbol{x}_*}\end{bmatrix}\right) \tag{5}$$

where $\boldsymbol{K}_{\boldsymbol{x}_*} = \left[k(\boldsymbol{x}_*, \boldsymbol{x}_1), ..., k(\boldsymbol{x}_*, \boldsymbol{x}_N)\right]^{\mathrm{T}}$, $k_{\boldsymbol{x}_*} = k(\boldsymbol{x}_*, \boldsymbol{x}_*)$

Then, the distribution $p(f_*|\boldsymbol{X}, \boldsymbol{x}_*, \boldsymbol{f})$ can be expressed as

$$\begin{aligned} &p(f_*|\boldsymbol{X}, \boldsymbol{x}_*, \boldsymbol{f})\\ &= N\left(\boldsymbol{K}_{\boldsymbol{x}_*}^{\mathrm{T}}\boldsymbol{K}^{-1}(\boldsymbol{f}-\boldsymbol{m}) + m_{\boldsymbol{x}_*}, k_{\boldsymbol{x}_*} - \boldsymbol{K}_{\boldsymbol{x}_*}^{\mathrm{T}}\boldsymbol{K}^{-1}\boldsymbol{K}_{\boldsymbol{x}_*}\right) \end{aligned} \tag{6}$$

Moreover, one can also obtain the posterior distribution $p(\boldsymbol{f}|\boldsymbol{X},\boldsymbol{Y})$ by Bayesian rules.

$$p(\boldsymbol{f}|\boldsymbol{X},\boldsymbol{Y}) = \frac{p(\boldsymbol{Y}|\boldsymbol{f})\,p(\boldsymbol{f}|\boldsymbol{X})}{p(\boldsymbol{Y}|\boldsymbol{X})} \tag{7}$$

where

$$p(\boldsymbol{Y}|\boldsymbol{f}) = \prod_{h=1}^{N} p(y_h|f_h) = \prod_{h=1}^{N} \Phi(y_h f_h)$$

$$p(\boldsymbol{Y}|\boldsymbol{X}) = \int p(\boldsymbol{f}|\boldsymbol{X})\,p(\boldsymbol{Y}|\boldsymbol{f})\mathrm{d}\boldsymbol{f}$$

The distribution of latent variable f_* can be obtained by introducing the Eqs. (6)-(7) into Eq. (2). Subsequently, the probability that the class label y_* of sample $\boldsymbol{x}_*$ belongs to +1 is

$$P(y_* = +1|\boldsymbol{X},\boldsymbol{Y},\boldsymbol{x}_*) = \int p(y_*|f_*)\,p(f_*|\boldsymbol{X},\boldsymbol{Y},\boldsymbol{x}_*)\mathrm{d}f_* \tag{8}$$

Unfortunately, since Eqs. (2) and (8) have no analytical solutions, it is necessary to adopt the analytical approximation methods to solve. Laplace and Expectation Propagation algorithms are two commonly used approximation methods, among which Laplace method has advantages over Expectation Propagation in keeping the balance of classification accuracy and computation time. Therefore, this research adopts the Laplace algorithm to obtain the approximate solution of the above integrals.

By performing a second-order Taylor expansion on the $\log\{p(\boldsymbol{f}|\boldsymbol{X},\boldsymbol{Y})\}$ at $\hat{\boldsymbol{f}}$ which maximizes the posterior distribution, Laplace method can gain an approximate Gaussian distribution $q(\boldsymbol{f}|\boldsymbol{X},\boldsymbol{Y})$ of the posterior distribution $p(\boldsymbol{f}|\boldsymbol{X},\boldsymbol{Y})$, i.e.

$$p(\boldsymbol{f}|\boldsymbol{X},\boldsymbol{Y}) \approx q(\boldsymbol{f}|\boldsymbol{X},\boldsymbol{Y}) = N\left(\hat{\boldsymbol{f}}, \left(\boldsymbol{K}^{-1} + \boldsymbol{U}\right)^{-1}\right) \tag{9}$$

where $\boldsymbol{U}$ represents the negative Hessian matrix of $\log\{p(\boldsymbol{f}|\boldsymbol{X},\boldsymbol{Y})\}$.

Therefore, Eq. (2) can be approximately expressed as

$$\begin{aligned} &p(f_*|\boldsymbol{X},\boldsymbol{Y},\boldsymbol{x}_*) \approx q(f_*|\boldsymbol{X},\boldsymbol{Y},\boldsymbol{x}_*) = N(\mu_*, \sigma_*^2)\\ &= N\left(\boldsymbol{K}_{\boldsymbol{x}_*}\boldsymbol{K}^{-1}\hat{\boldsymbol{f}}, k_{\boldsymbol{x}_*} - \boldsymbol{K}_{\boldsymbol{x}_*}{}^{\mathrm{T}}\left(\boldsymbol{K}+\boldsymbol{U}^{-1}\right)^{-1}\boldsymbol{K}_{\boldsymbol{x}_*}\right) \end{aligned} \tag{10}$$

Furthermore, the parameters σ_f and l in the covariance function SE are obtained using maximum likelihood estimation.

$$\begin{aligned} \max L(\sigma_f, l) = &-\frac{1}{2}\hat{\boldsymbol{f}}^{\mathrm{T}}\boldsymbol{K}^{-1}\hat{\boldsymbol{f}} + \log\left\{p(\boldsymbol{Y}|\hat{\boldsymbol{f}})\right\}\\ &-\frac{1}{2}\log\left|\boldsymbol{I} + \boldsymbol{U}^{1/2}\boldsymbol{K}\boldsymbol{U}^{1/2}\right| \end{aligned} \tag{11}$$

where $\boldsymbol{I}$ denotes the identity matrix.

Subsequently, the probability of class label y_* belonging to +1 is

$$\begin{aligned} &P(y_* = +1|\boldsymbol{X},\boldsymbol{Y},\boldsymbol{x}_*)\\ &\approx \int p(y_*|f_*)\,q(f_*|\boldsymbol{X},\boldsymbol{Y},\boldsymbol{x}_*)\mathrm{d}f_*\\ &= \int \sigma(f_*)\,q(f_*|\boldsymbol{X},\boldsymbol{Y},\boldsymbol{x}_*)\mathrm{d}f_* = \Phi\left(\mu_*/\sqrt{1+\sigma_*^2}\right) \end{aligned} \tag{12}$$

where $\sigma(\cdot)$ is the response function which maps f_* to interval [0, 1]. In this research, we select the cumulative density function of standard normal distribution as the response function.

$$\sigma(f) = \frac{1}{\sqrt{2\pi}}\int_{-\infty}^{f}\exp\left(-\frac{1}{2}u^2\right)du$$

Obviously, if the probability in Eq. (12) is greater than 0.5, y_* is 1, i.e. structure is safe, otherwise y_* is -1 and structure fails.

2.2 Importance sampling for reliability analysis

Importance sampling technique aims at increasing the number of samples in the failure domain and reducing the number of samples required for reliability evaluation. After a Gaussian process classifier is established, the failure probability estimated using importance sampling is expressed as (Yun *et al.* 2017, Barkhori *et al.* 2018)

$$\begin{aligned} \hat{P}_f = &\int_{\hat{G}(\boldsymbol{x})\le 0} f_X(\boldsymbol{x})\mathrm{d}\boldsymbol{x} = \int I_y(\boldsymbol{x})\frac{f_X(\boldsymbol{x})}{h(\boldsymbol{x})}h(\boldsymbol{x})\mathrm{d}\boldsymbol{x}\\ &\approx \frac{1}{N_{\mathrm{IS}}}\sum_{i=1}^{N_{\mathrm{IS}}} I_y(\boldsymbol{x}_i)\frac{f_X(\boldsymbol{x}_i)}{h(\boldsymbol{x}_i)} \end{aligned} \tag{13}$$

where N_{IS} represents the number of samples from the

optimal importance sampling PDF $h(\boldsymbol{x})$, and $I_y(\boldsymbol{x})$ denotes the failure indicator function, that is, if the class label y is equal to -1, $I_y(\boldsymbol{x})$ is 1, otherwise $I_y(\boldsymbol{x})$ is 0.

The corresponding variance and coefficient of variation of $\hat{P}_f$ are

$$\mathrm{var}\left(\hat{P}_f\right)=\frac{1}{N_{\mathrm{IS}}}\left(\frac{1}{N_{\mathrm{IS}}}\sum_{i=1}^{N_{\mathrm{IS}}}I_y\left(\boldsymbol{x}_i\right)\left(\frac{f_X\left(\boldsymbol{x}_i\right)}{h\left(\boldsymbol{x}_i\right)}\right)^2-\hat{P}_f^2\right) \tag{14}$$

$$\delta_{\hat{P}_f}=\sqrt{\mathrm{var}\left(\hat{P}_f\right)}\Big/\hat{P}_f \tag{15}$$

3. AGPC-IS for structures with discontinuous response and small failure probability

Taking into consideration the classification uncertainty, the sampling uniformity and the regional classification accuracy improvement, this section proposes an innovative adaptive DoE strategy based on GPC to avoid unnecessary calls of performance function. On this foundation, a novel reliability analysis method AGPC-IS, fusing with IS based on adaptive kernel density estimation, is developed for structures with discontinuous response and small failure probability. In addition, a new and more accurate stopping criterion for AGPC-IS is also developed.

3.1 Existing GPC-based adaptive DoE strategies

3.1.1 Most probable point

In GPC, the most probable point (MPP) refers to the sample with a classification probability of 0.5 and the greatest contribution to the failure probability. Therefore, the fitting accuracy of Gaussian process classifier in the vicinity of MPP has a significant influence on the accuracy of the estimated failure probability. Consequently, Peng *et al.* (2014) regard the MPP as the new training sample for improving the accuracy of Gaussian process classifier. The MPP can be obtained approximately by

$$\begin{cases}\max & f_X\left(\boldsymbol{x}\right)\\ \text{s.t.} & p\left(y=+1\middle|\boldsymbol{X},\boldsymbol{Y},\boldsymbol{x}\right)<0.5\\ & \boldsymbol{x}\in S_\Omega\end{cases} \tag{16}$$

where S_Ω is a set of Monte Carlo random samples.

3.1.2 Most easily misclassified point

According to Eq. (12), it can be easily concluded that the closer the classification probability of sample is to 0.5, the higher risk of being misclassified its class label has. Accordingly, Kapoor *et al.* (2009) and Rodrigues *et al.* (2014) define the most easily misclassified point, which is termed as MEMP in this paper, as the new training sample. Obviously, the point satisfying the Eq. (17) is the MEMP.

$$\boldsymbol{x}=\arg\min\Phi\left(\frac{|\mu|}{\sqrt{1+\sigma^2}}\right) \tag{17}$$

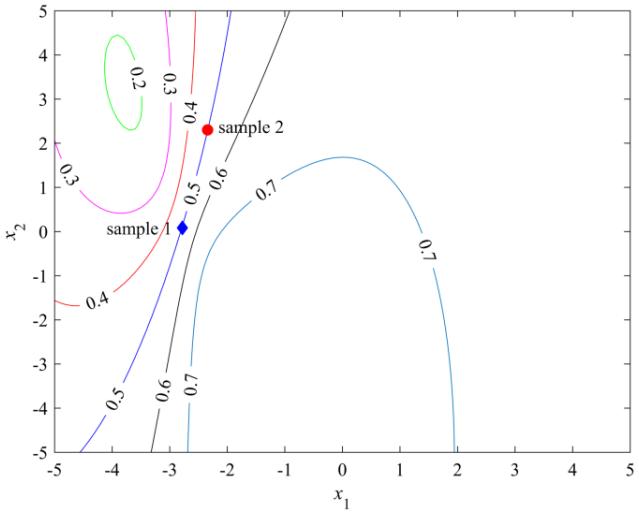

Fig. 1 The contour distribution of classification probability

Eq. (17) takes into consideration the posterior mean and the posterior variance of latent variable, and it is analogous to the learning function U proposed by Echard *et al.* (2011) in the Kriging-based reliability analysis.

3.2 The proposed adaptive DoE strategy

The adaptive DoE strategies based on MPP and MEMP ignore the sampling uniformity when determining the new training sample, resulting in aggregation or overlap of the training samples in DoE. Regrettably, this defect has little improvement on the accuracy of Gaussian process classifier while causing redundant evaluations of performance function. Furthermore, the above two strategies only consider improving the classification accuracy of a single sample, rather than refining that of the region near the determined training sample. This defect, as illustrated in Fig. 1, often makes some of more valuable samples overlooked. Fig. 1 shows the contour distribution of classification probability, where the classification probabilities of sample 1 (denoted by blue diamond) and sample 2 (denoted by red circle) are both approximately 0.5. However, the contours near sample 2 are sparser than those near sample 1, that is, the gradient of classification probability of sample 2 is smaller, which means that the class labels of samples near sample 2 are more uncertain than those near sample 1. Therefore, taking sample 2 as the new training sample can improve the accuracy of Gaussian process classifier to a greater extent.

To overcome these two defects, the Euclidean distance and the gradient of classification probability are introduced in this paper. In addition, according to GPC, the samples with a classification probability of 0.5 have the greatest impact on the accuracy improvement of Gaussian process classifier and they should be considered as the candidate samples. However, it is very difficult and unrealistic to directly generate or select the samples with a classification probability of 0.5. Therefore, this paper adopts the Markov Chain Monte Carlo (MCMC) (Au 2016) to generate N_{CS} samples satisfying the Eq. (18) and regards them as the candidate samples.

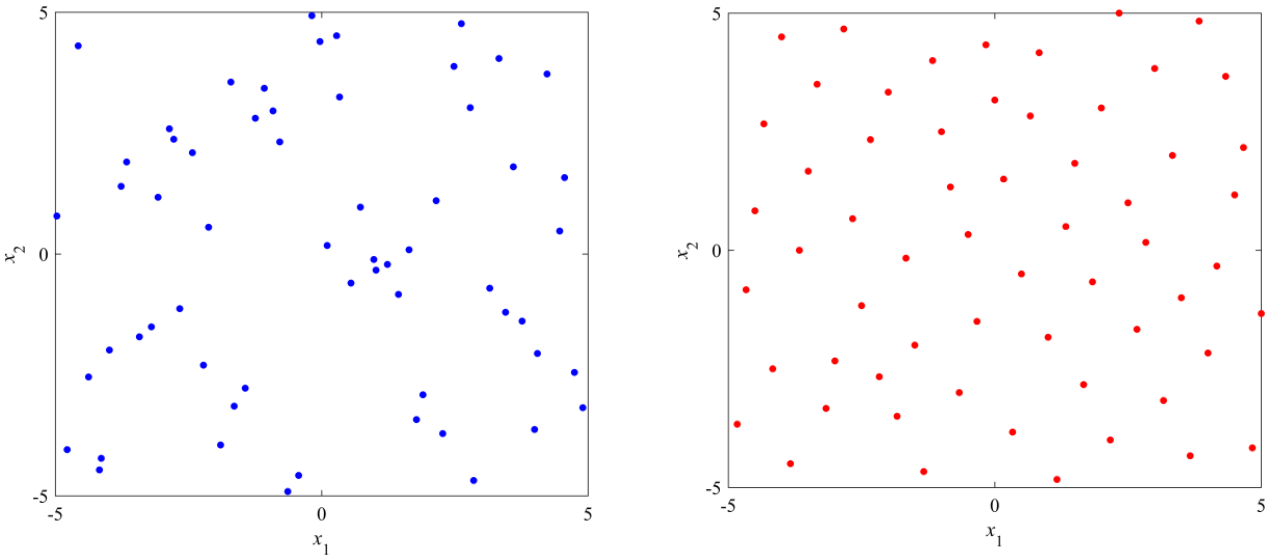

(a) LHS (b) IHS

Fig. 2 Distribution of samples obtained by LHS and IHS

$$\left|p\left(y=+1\middle|\boldsymbol{X},\boldsymbol{Y},\boldsymbol{x}\right)-0.5\right|\le\left[\varepsilon\right] \tag{18}$$

where $[\varepsilon]$ is set to 0.01.

The Euclidean distance is adopted to ensure the sampling uniformity and it can be obtained by

$$d=\sqrt{\sum_{h=1}^{M}\left(x_s^h-x_t^h\right)^2} \tag{19}$$

where $\boldsymbol{x}_s$ and $\boldsymbol{x}_t$ represent the candidate sample and the existing training sample, respectively.

The gradient of classification probability is utilized to identify a more valuable sample. According to Eq. (12), the gradient of classification probability of $\boldsymbol{x}$ is expressed as

$$\begin{aligned}Grad\left(\boldsymbol{x}\right)&=\left\|\Phi'\left(\mu/\sqrt{1+\sigma^2}\right)\right\|_2\\&=\left\|\varphi\left(\frac{\mu}{\sqrt{1+\sigma^2}}\right)\frac{2\mu'\left(1+\sigma^2\right)-\mu\left(\sigma^2\right)'}{2\left(1+\sigma^2\right)^{1.5}}\right\|_2\end{aligned} \tag{20}$$

where $\varphi(\cdot)$ denotes the PDF of standard normal distribution.

Unfortunately, it has difficulty in obtaining the gradient of classification probability in the framework of GPC. For this reason, this research proposes to introduce the Kriging surrogate model to obtain the approximate solution of gradient. As an accurate regression-based interpolation technique, the Kriging model can provide the prediction and its corresponding derivative. It should be paid special attention that instead of solving gradient by directly modeling classification probability function $\Phi(\boldsymbol{x})$ ($\Phi(x)=\left(\mu(x)/\sqrt{1+\sigma^2(x)}\right)$), the Kriging surrogate models of posterior mean function $\mu(\boldsymbol{x})$ and posterior variance function $\sigma^2(\boldsymbol{x})$ are established to obtain the gradient. This is mainly because the classification probabilities of samples in the entire sampling space gradually approach 0 or 1 as the training samples in DoE increase. That is to say, $\Phi(\boldsymbol{x})$ presents a discontinuous trend on the whole, which easily leads to the poor accuracy of its corresponding Kriging surrogate model. Fortunately, $\mu(\boldsymbol{x})$ and $\sigma^2(\boldsymbol{x})$ are both continuous functions and can be well simulated by Kriging model. Next, the processes of establishing the Kriging model of $\mu(\boldsymbol{x})$ and obtaining its prediction and derivative are elaborately introduced. Firstly, a Gaussian process classifier is constructed using the existing training samples in DoE. Subsequently, N_L random samples are extracted by the improved distributed hypercube sampling (IHS) (Beachkofski and Grandhi 2002) and their corresponding posterior mean values are obtained by the constructed classifier. The IHS is an improvement of Latin hypercube sampling (LHS), and samples obtained using IHS are more evenly distributed than those generated by LHS. Fig. 2 describes the advantage of IHS over LHS.

Then, the Kriging surrogate model of posterior mean function $\mu(\boldsymbol{x})$ can be expressed as (Gao *et al.* 2012, Vahedi *et al.* 2018, Qin *et al.* 2019)

$$\mu\left(\boldsymbol{x}\right)=\boldsymbol{g}\left(\boldsymbol{x}\right)^{\mathrm{T}}\boldsymbol{\beta}+z\left(\boldsymbol{x}\right) \tag{21}$$

where $g(\boldsymbol{x})^{\mathrm{T}}\boldsymbol{\beta}$ is the regression part and $z(\boldsymbol{x})$ is a Gaussian stochastic process.

Afterwards, the prediction and derivative of posterior mean of sample $\boldsymbol{x}$ can be obtained by

$$\hat{\mu}\left(\boldsymbol{x}\right)=\hat{\beta}_\mu+\boldsymbol{r}\left(\boldsymbol{x}\right)\boldsymbol{R}^{-1}\left(\boldsymbol{Y}_\mu-\boldsymbol{G}\hat{\beta}_\mu\right) \tag{22}$$

$$\begin{aligned}\hat{\mu}'\left(\boldsymbol{x}\right)&=\left[\partial\hat{\mu}\left(\boldsymbol{x}\right)/\partial\boldsymbol{x}^1,...,\partial\hat{\mu}\left(\boldsymbol{x}\right)/\partial\boldsymbol{x}^M\right]^{\mathrm{T}}\\&=\boldsymbol{J}_g\left(\boldsymbol{x}\right)^{\mathrm{T}}\left(\boldsymbol{G}^{\mathrm{T}}\boldsymbol{R}^{-1}\boldsymbol{G}\right)^{-1}\boldsymbol{G}^{\mathrm{T}}\boldsymbol{R}^{-1}\boldsymbol{Y}_\mu\\&\quad+\boldsymbol{J}_r\left(\boldsymbol{x}\right)^{\mathrm{T}}\boldsymbol{R}^{-1}\left(\boldsymbol{Y}_\mu-\boldsymbol{G}\hat{\beta}_\mu\right)\end{aligned} \tag{23}$$

where

$$\hat{\beta}_{\mu}=\left(\boldsymbol{G}^{\mathrm{T}}\boldsymbol{R}^{-1}\boldsymbol{G}\right)^{-1}\boldsymbol{G}^{\mathrm{T}}\boldsymbol{R}^{-1}\boldsymbol{Y}_{\mu}$$
$$\boldsymbol{G}=\left[\boldsymbol{g}\left(\boldsymbol{x}_1\right),...,\boldsymbol{g}\left(\boldsymbol{x}_{N_{\mathrm{L}}}\right)\right]^{\mathrm{T}}$$
$$\boldsymbol{R}=\left(R\left(\boldsymbol{x}_i,\boldsymbol{x}_j;\boldsymbol{\theta}\right)\right)_{N_{\mathrm{L}}\times N_{\mathrm{L}}}$$
$$R\left(\boldsymbol{x}_i,\boldsymbol{x}_j;\boldsymbol{\theta}\right)=\exp\sum_{k=1}^{M}\left[-\theta_k\left(x_i^k-x_j^k\right)^2\right]$$
$$\boldsymbol{Y}_{\mu}=\left[\mu\left(\boldsymbol{x}_1\right),...,\mu\left(\boldsymbol{x}_{N_{\mathrm{L}}}\right)\right]^{\mathrm{T}}$$
$$\boldsymbol{r}\left(\boldsymbol{x}\right)=\left[R\left(\boldsymbol{x},\boldsymbol{x}_1;\boldsymbol{\theta}\right),...,R\left(\boldsymbol{x},\boldsymbol{x}_{N_{\mathrm{L}}};\boldsymbol{\theta}\right)\right]$$

Moreover, $\boldsymbol{J}_g(\boldsymbol{x})$ and $\boldsymbol{J}_r(\boldsymbol{x})$ are the Jacobian matrices of $\boldsymbol{g}(\boldsymbol{x})$ and $\boldsymbol{r}(\boldsymbol{x})$, respectively. For more detailed theory and details about the Kriging model, please refer to the publications (Gao *et al*. 2012, Vahedi *et al*. 2018, Qin *et al*. 2019).

Similarly, the prediction and derivative of the posterior variance of sample $\boldsymbol{x}$ are

$$\hat{\sigma}^2\left(\boldsymbol{x}\right)=\hat{\beta}_{\sigma^2}+\boldsymbol{r}\left(\boldsymbol{x}\right)\boldsymbol{R}^{-1}\left(\boldsymbol{Y}_{\sigma^2}-\boldsymbol{G}\hat{\beta}_{\sigma^2}\right) \tag{24}$$

$$\begin{aligned}\left(\hat{\sigma}^2\left(\boldsymbol{x}\right)\right)'&=\left[\frac{\partial\hat{\sigma}^2\left(\boldsymbol{x}\right)}{\partial\boldsymbol{x}^1},...,\frac{\partial\hat{\sigma}^2\left(\boldsymbol{x}\right)}{\partial\boldsymbol{x}^M}\right]^{\mathrm{T}}\\&=\boldsymbol{J}_g\left(\boldsymbol{x}\right)^{\mathrm{T}}\left(\boldsymbol{G}^{\mathrm{T}}\boldsymbol{R}^{-1}\boldsymbol{G}\right)^{-1}\boldsymbol{G}^{\mathrm{T}}\boldsymbol{R}^{-1}\boldsymbol{Y}_{\sigma^2}\\&\quad+\boldsymbol{J}_r\left(\boldsymbol{x}\right)^{\mathrm{T}}\boldsymbol{R}^{-1}\left(\boldsymbol{Y}_{\sigma^2}-\boldsymbol{G}\hat{\beta}_{\sigma^2}\right)\end{aligned} \tag{25}$$

where

$$\hat{\beta}_{\sigma^2}=\left(\boldsymbol{G}^{\mathrm{T}}\boldsymbol{R}^{-1}\boldsymbol{G}\right)^{-1}\boldsymbol{G}^{\mathrm{T}}\boldsymbol{R}^{-1}\boldsymbol{Y}_{\sigma^2}$$

$$\boldsymbol{Y}_{\sigma^2}=\left[\sigma^2\left(\boldsymbol{x}_1\right),...,\sigma^2\left(\boldsymbol{x}_{N_{\mathrm{L}}}\right)\right]^{\mathrm{T}}$$

Bring the Eqs. (22)-(25) into Eq. (20), the gradient of classification probability of sample $\boldsymbol{x}$ can be obtained approximately by

$$Grad\left(\boldsymbol{x}\right)\approx\left\|\varphi\left(\frac{\hat{\mu}\left(\boldsymbol{x}\right)}{\sqrt{1+\hat{\sigma}^2\left(\boldsymbol{x}\right)}}\right)\frac{2\hat{\mu}'\left(\boldsymbol{x}\right)\left(1+\hat{\sigma}^2\left(\boldsymbol{x}\right)\right)-\hat{\mu}\left(\boldsymbol{x}\right)\left(\hat{\sigma}^2\left(\boldsymbol{x}\right)\right)'}{2\left(1+\hat{\sigma}^2\left(\boldsymbol{x}\right)\right)^{1.5}}\right\|_2 \tag{26}$$

Therefore, the sample with a higher probability of being misclassified, a lower gradient of classification probability and a greater distance from the existing training samples should be added to the DoE. Obviously, the new training sample is defined as

$$\boldsymbol{x}_{new}=\arg\max\left\{\bar{\Phi}\bar{G}\bar{d}\right\} \tag{27}$$

where $\bar{\Phi}$, $\bar{G}$ and $\bar{d}$ are the normalized values of $\Phi(\boldsymbol{x})$, $Grad(\boldsymbol{x})$ and $d_{\min}$ (the shortest distance from all the training samples in DoE), respectively, and they are expressed as

$$\begin{aligned}\bar{\Phi}&=\frac{\left|\left|\Phi(\boldsymbol{x})-0.5\right|-\max\left(\left|\Phi(\boldsymbol{x})-0.5\right|\right)\right|}{\max\left(\left|\Phi(\boldsymbol{x})-0.5\right|\right)-\min\left(\left|\Phi(\boldsymbol{x})-0.5\right|\right)}\\\bar{d}&=\frac{d_{\min}-\min\left(d_{\min}\right)}{\max\left(d_{\min}\right)-\min\left(d_{\min}\right)}\\\bar{G}&=\frac{\left|Grad\left(\boldsymbol{x}\right)-\max\left(Grad\left(\boldsymbol{x}\right)\right)\right|}{\max\left(Grad\left(\boldsymbol{x}\right)\right)-\min\left(Grad\left(\boldsymbol{x}\right)\right)}\end{aligned} \tag{28}$$

The purpose of normalizing $\bar{\Phi}$, $\bar{G}$ and $\bar{d}$ is to eliminate the influence of the magnitude difference between them.

3.3 Importance sampling based on adaptive kernel density estimation

The construction of optimal importance sampling PDF $h(\boldsymbol{x})$ is a key issue in IS. Since the optimal $h(\boldsymbol{x})$ involves the real failure probability, it cannot be obtained in engineering practice. To this end, various construction methods of quasi-optimal $\hat{h}\left(\boldsymbol{x}\right)$ are proposed, among which those combining kernel density estimation or adaptive kernel density estimation are superior to other methods (Au and Beck 1999, Yang *et al.* 2018). Therefore, the adaptive kernel density estimation is employed to construct $\hat{h}\left(\boldsymbol{x}\right)$ in this paper. First, N_{k} failure samples are generated using MCMC, and then $\hat{h}\left(\boldsymbol{x}\right)$ can be obtained by

$$\hat{h}\left(\boldsymbol{x}\right)=\frac{1}{N_{\mathrm{k}}}\sum_{i=1}^{N_{\mathrm{k}}}\frac{1}{\left(\lambda_i\omega\right)^M}K\left(\frac{\boldsymbol{x}-\boldsymbol{x}_i}{\lambda_i\omega}\right) \tag{29}$$

where λ_i is the bandwidth factors, ω is the bandwidth and N_{k} usually takes as 1500. $K(\cdot)$ denotes the kernel PDF and this paper employs the widely used PDF of Gaussian distribution as $K(\cdot)$, i.e. $K(\cdot)$ is expressed as

$$K\left(\boldsymbol{x}\right)=\frac{1}{\sqrt{\left(2\pi\right)^M\left|\Sigma\right|}}\exp\left(-\frac{\boldsymbol{x}^{\mathrm{T}}\Sigma^{-1}\boldsymbol{x}}{2}\right) \tag{30}$$

where Σ represents the covariance of N_{k} failure samples.

Furthermore, the bandwidth factors λ_i and the bandwidth ω can be obtained respectively by

$$\lambda_i=\left(\left(\prod_{l=1}^{N_{\mathrm{k}}}f_X\left(\boldsymbol{x}_l\right)\right)^{1/N_{\mathrm{k}}}\Big/f_X\left(\boldsymbol{x}_i\right)\right)^{\alpha} \tag{31}$$

$$\omega=\arg\min\left(\frac{1}{N_{\mathrm{k}}}\sum_{i=1}^{N_{\mathrm{k}}}\frac{f_X\left(\boldsymbol{x}_i\right)}{h_{-i}\left(\boldsymbol{x}_i\right)}\right) \tag{32}$$

where α is the sensitivity factor and it is usually set to 0.5. The $h_{-i}(\boldsymbol{x})$ denotes the kernel density estimation by the leave-one-out cross validation, i.e. $h_{-i}(\boldsymbol{x})$ is obtained using all failure samples except $\boldsymbol{x}_i$.

3.4 Stopping criterion

Existing stopping criteria which are available for the reliability analysis of structures with discontinuous response

mainly include three types. However, they are unacceptable in engineering applications due to some inherent defects.

1) Since the finite element analysis (FEA) of structure is very time-consuming, the iterative process terminates as soon as the total number of performance function evaluations reaches a certain value $N_{\max}$ (Li *et al.* 2018). Obviously, the estimated failure probability is inaccurate if $N_{\max}$ is small. Conversely, it will cause unnecessary performance function evaluations if $N_{\max}$ is large.

2) The relative error of estimated failure probability or the change rate of class labels of N_{MC} Monte Carlo samples in the i-1th and ith iterations is less than a specified threshold δ (Peng *et al.* 2014). Nevertheless, this stopping criterion can be easily satisfied if the new training sample makes little improvement on the classifier, i.e. the iterative process terminates in advance. Furthermore, this criterion is not applicable to the structures involving small failure probability.

$$\frac{\left|\hat{P}_f^i-\hat{P}_f^{i-1}\right|}{\hat{P}_f^i}\le\delta \quad \text{or} \quad \frac{\sum_{l=1}^{N_{\mathrm{MC}}}\left|I_y^i(\boldsymbol{x}_l)-I_y^{i-1}(\boldsymbol{x}_l)\right|}{N_{\mathrm{MC}}}\le\delta \tag{33}$$

3) Basudhar and Missoum (2008) propose using an exponential curve to fit the Eq. (33) and they define the stopping criterion as

$$\begin{cases}\dfrac{\sum_{l=1}^{N_{\mathrm{MC}}}\left|I_y^i(\boldsymbol{x}_l)-I_y^{i-1}(\boldsymbol{x}_l)\right|}{N_{\mathrm{MC}}}\approx Ae^{Bi}\le\varepsilon_1\\ \left|ABe^{Bi}\right|<\varepsilon_2\end{cases} \tag{34}$$

However, the thresholds ε_1 and ε_2 are different for different problems, i.e. it has difficulty in determining their specific values. Moreover, this criterion is also not applicable to the structures involving small failure probability.

To overcome these defects, a novel stopping criterion is proposed in this research. As is known, the Gaussian process classifier gradually becomes accurate as the iteration progresses. Simultaneously, the extent of improvement of classifier also gradually decreases. This means that the estimation of failure probability gradually tends to be stable. Consequently, an innovative convergence criterion based on this stability is proposed, which is expressed as

$$\varepsilon=\max_{a=i,i+1,\cdots,i+N_{\mathrm{P}}-1}\left\{\left|\frac{\hat{P}_f^a-\dfrac{1}{N}\sum_{j=i}^{i+N_{\mathrm{P}}-1}\hat{P}_f^j}{\dfrac{1}{N_{\mathrm{P}}}\sum_{j=i}^{i+N_{\mathrm{P}}-1}\hat{P}_f^j}\right|\right\}\le[\delta] \tag{35}$$

where $\frac{1}{N_{\mathrm{P}}}\sum_{j=i}^{i+N_{\mathrm{P}}-1}\hat{P}_f^j$ denotes the average of estimated failure probabilities obtained from the ith iteration and subsequent N_{P}-1 iterations. $\hat{P}_f^a$ is one of the N_{P} estimations of failure probability. The parameter ε is defined as the maximum relative stability and it is employed to characterize the extent of stability of estimated failure probability. Obviously, ε should be as small as possible. The estimation of failure probability can be considered to be steady and the iteration terminates once ε is less than or equal to a certain threshold $[\delta]$. In this research, $[\delta]$ is set to 0.03. Furthermore, the parameter N_{P} can neither be too large nor too small, otherwise the efficiency will decrease or the stopping criterion will be reached prematurely. In this research, N_{P} is taken as 10.

The new stopping criterion is analogous to Eq. (33) and it can be regarded as an improvement of Eq. (33). Compared with Eq. (33), the proposed convergence criterion effectively avoids the early termination of iteration and can also obtain an accurate estimation of failure probability.

Furthermore, the relative error of $\hat{P}_f$ is determined as

$$\varepsilon_{\hat{P}_f}=\frac{\left|\hat{P}_f-\hat{P}_f^{\mathrm{IS}}\right|}{\hat{P}_f^{\mathrm{IS}}} \tag{36}$$

where $\hat{P}_f^{\mathrm{IS}}$ is calculated by AKDE-based IS (termed as AKDE-IS in this research). In this research, $\hat{P}_f^{\mathrm{IS}}$ is regarded as the "true" failure probability of the structure.

3.5 The process of AGPC-IS

This subsection constructs an innovative adaptive reliability analysis method AGPC-IS integrating GPC with IS for the structures with discontinuous response and small failure probability. The main procedures of AGPC-IS are listed as follows and the process is presented in Fig. 3.

Step 1 Adopt the Nataf transformation to map the original random vector space into the mutually independent standard normal space. The main reason for using the Nataf transformation is that it is of high calculation accuracy, wide application range and unnecessary to know the joint probability density function $f_X(\boldsymbol{x})$ of $\boldsymbol{x}$. Then, generate N initial training samples $\boldsymbol{S}_{\mathrm{DoE}}=[\boldsymbol{x}_1, \boldsymbol{x}_2, \ldots, \boldsymbol{x}_N]$ within the standard normal space using LHS, and obtain their corresponding real class labels $\boldsymbol{Y}_{\mathrm{DoE}}=[y_1, y_2, \ldots, y_N]$.

Step 2 Construct a Gaussian process classifier using existing DoE. Subsequently, extract N_{L} random samples by IHS and calculate the posterior means and the posterior variances of their corresponding latent variables. Then, establish the Kriging surrogate models of posterior mean function $\mu(\boldsymbol{x})$ and posterior variance function $\sigma^2(\boldsymbol{x})$, respectively. According to our experience, the Kriging surrogate models with good accuracy can be obtained by taking N_{L} as 150.

Step 3 Generate N_{k} failure samples using MCMC and construct the quasi-optimal $\hat{h}(x)$ by adaptive kernel density estimation. Then, estimate the failure probability by IS. As long as the stopping criterion in Eq. (35) is not satisfied, proceed to the next step, otherwise skip to Step 5. According to the publication (Yang *et al.* 2018), more than 1000 failure samples are needed for obtaining an accurate quasi-optimal PDF $\hat{h}(x)$. In addition, it should be noted that these failure samples are generated based on the current Gaussian process classifier instead of performing the performance function evaluations.

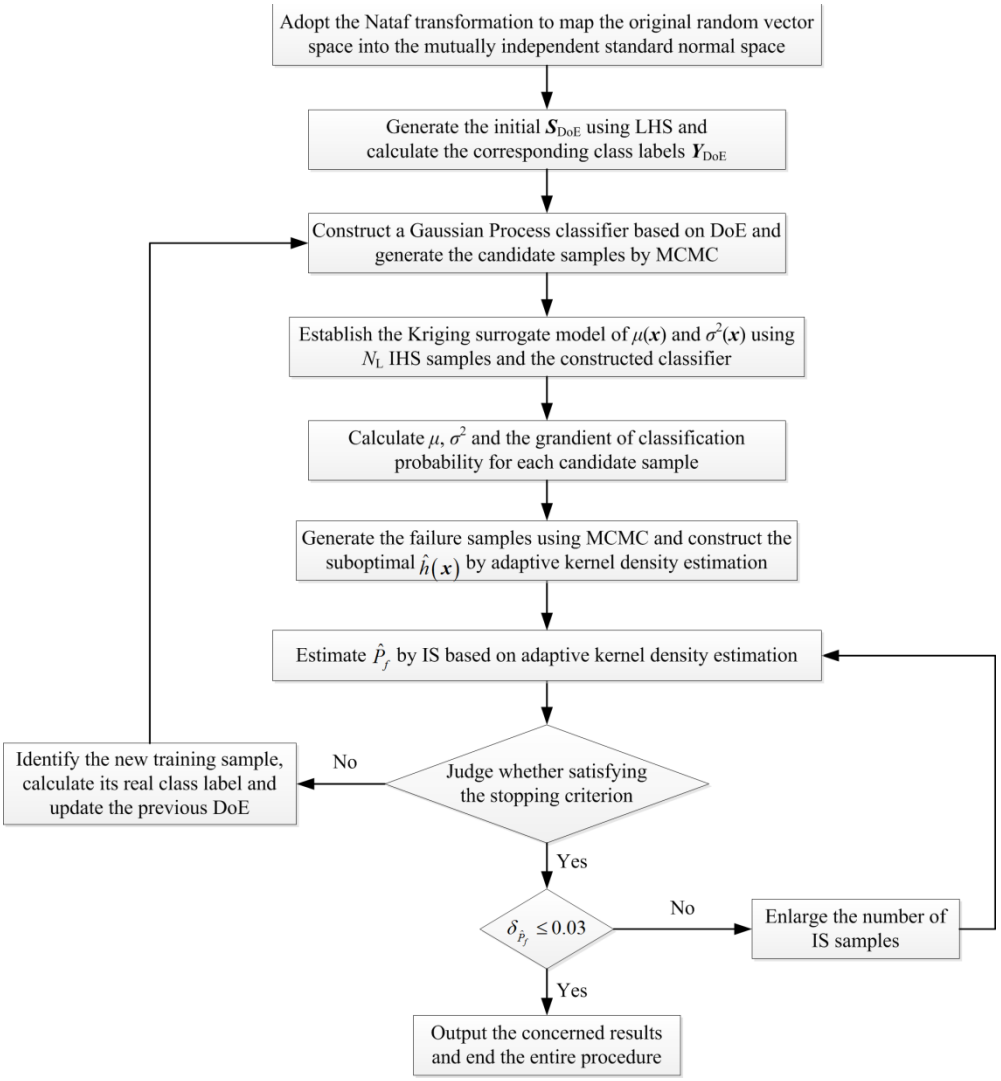

Fig. 3 The process of AGPC-IS

Step 4 Select the new training sample from the N_{CS} candidate samples generated by MCMC according to the proposed adaptive DoE strategy in 3.2 at each iteration and add it to DoE. Subsequently, update the Gaussian process classifier and the Kriging surrogate models, i.e. return to Step 2.

Step 5 Estimate the coefficient of variation of failure probability. If $\delta_{\hat{P}_f} \le 0.03$ is satisfied, terminate the adaptive iteration and output the estimation of some concerned results. Otherwise, increase the number of random samples obtained by IS and return to Step 3 until $\delta_{\hat{P}_f} \le 0.03$ is satisfied.

4. Verification and application

4.1 Piecewise function with two random variables

A piecewise function with discontinuous output, obtained from the fusion of the publications (Guan and Melchers 2001, Yuan *et al.* 2013), is taken as the first example. The discontinuity of its output under two random inputs and the segmentation boundary of sampling space are shown in Fig. 4. The piecewise function is expressed as

$$G(\boldsymbol{x}) = \begin{cases} -4 - \dfrac{4(x_1-1)^2}{25} - x_2 \\ \left((x_1-15)^2 + (x_2+5)^2 \ge 19.5^2\right); \\ 38 - \exp\left(-\dfrac{x_1^2}{10}\right) - \left(\dfrac{x_1}{5}\right)^4 + x_2 \\ \left((x_1-15)^2 + (x_2+5)^2 < 19.5^2\right) \end{cases} \tag{37}$$

where $x_1 \sim N(0,1)$, $x_2 \sim N(0,1)$ and they are mutually independent.

Twelve initial training samples extracted using LHS are employed to construct an initial Gaussian process classifier. The average results of 10 runs of GPC+MPP, GPC+MEMP and AGPC-IS are summarized in Table 1. The results of AKDE-IS are regarded as the "true" values and it needs 5×10^4 calculations of the piecewise function. The reliability analysis methods based on GPC are also compared with SVC-based one in publication (Pan and Dias *et al*. 2017) (called as ASVC in this paper) and the results of ASVC are

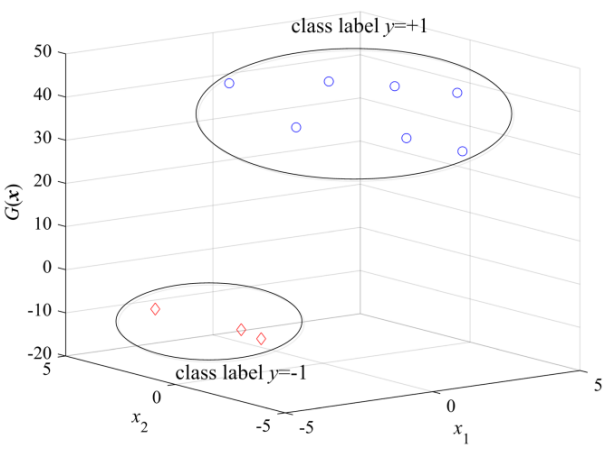

(a) discontinuous output

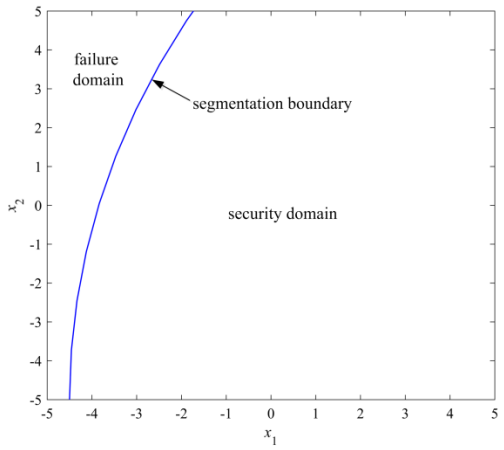

(b) segmentation boundary

Fig. 4 Characteristics of piecewise function

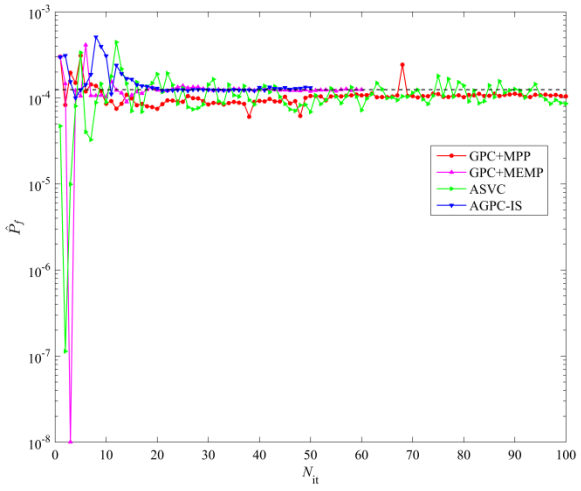

(a) Variations of $\hat{P}_f$ with N_{it}

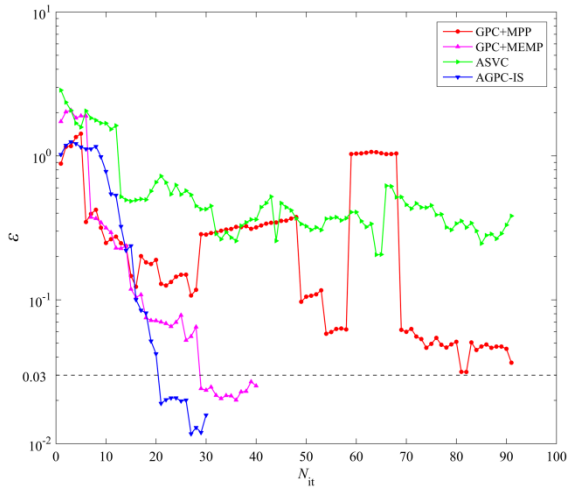

(b) Variations of ε with N_{it}

Fig. 5 Variations of $\hat{P}_f$ and ε with N_{it} using different methods

listed in Table 1. Moreover, GPC+MPP, GPC+MEMP and ASVC all take the samples generated by AKDE-IS as the candidate samples. Table 1 contains the following contents: the total calls of piecewise function N_{call}, the estimated failure probability $\hat{P}_f$ and corresponding coefficient of variation $\delta_{\hat{P}_f}$, the relative error $\varepsilon_{\hat{P}_f}$. Moreover, the variations of $\hat{P}_f$ and maximum relative stability ε with the number of iteration N_{it} obtained using different methods are clearly depicted in Fig. 5.

Table 1 Average results obtained by different methods

Method	N_{call}	$\hat{P}_f$ (10^{-4})	$\delta_{\hat{P}_f}$ (%)	$\varepsilon_{\hat{P}_f}$ (%)
AKDE-IS	5×10^4	1.246	1.40	-
GPC+MPP	>112	1.050	1.63	15.73
GPC+MEMP	52.57	1.217	1.35	2.33
ASVC	>112	1.134	1.44	8.99
AGPC-IS	42.06	1.228	1.39	1.44

Obviously, the results obtained by GPC+MEMP and AGPC-IS approach to the "true" failure probability, while those using GPC+MPP and ASVC deviate greatly from the "true" value. In addition, compared with GPC+MEMP, AGPC-IS requires fewer calls of piecewise function. In other words, AGPC-IS is superior in efficiency to other methods while satisfying the accuracy requirements of reliability analysis.

Furthermore, Fig. 6 shows the processes that the classification boundary estimated by different methods gradually converges to the segmentation boundary of the piecewise function. In Fig. 6, each column denotes the convergence process of GPC+MPP, GPC+MEMP, ASVC and AGPC-IS, respectively. Each row, containing 22, 32, 42 training samples respectively, compares the distribution of training samples in these methods. The black line represents the actual segmentation boundary, while the green line denotes the classification boundary predicted by GPC or SVC. Obviously, the training samples selected by GPC+MPP are too centralized and have little improvement on the accuracy of Gaussian process classifier, and the classification effect of ASVC is poor when only a small number of labeled samples are available. In addition, it can

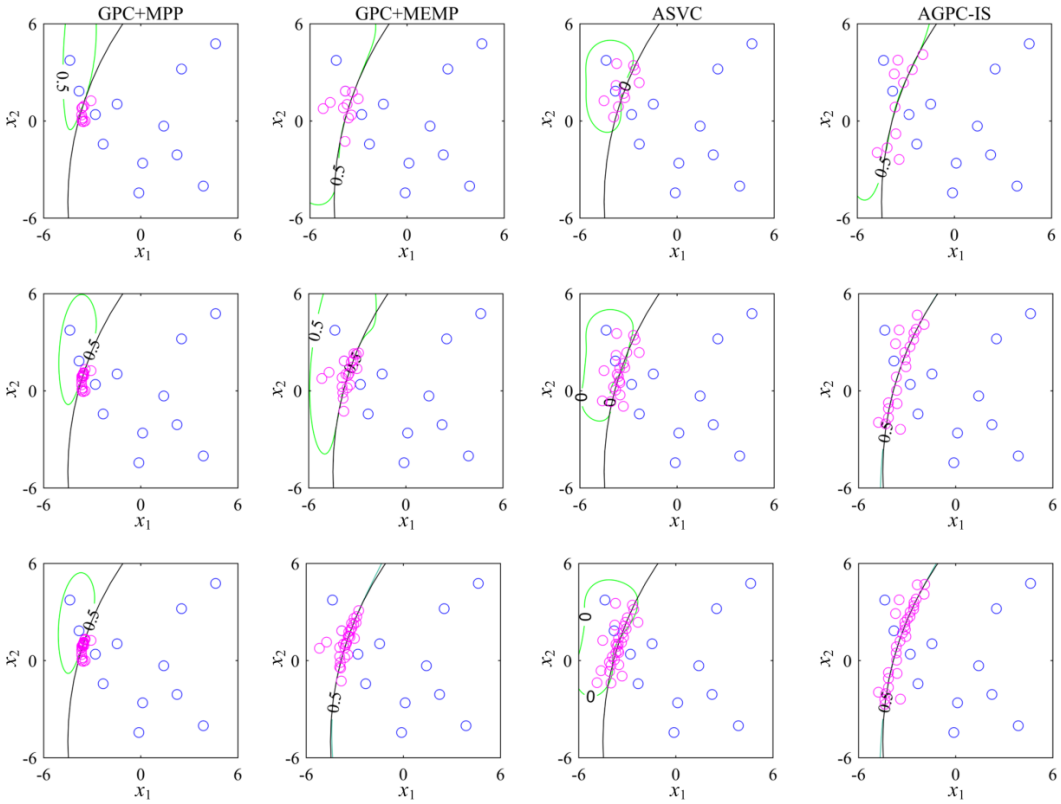

Fig. 6 Comparison of distribution of training samples and convergence process by different methods

be easily found that AGPC-IS can better converge to the real segmentation boundary of the piecewise function while sampling uniformly.

4.2 Arch structure with snap-through behavior

As a typical structure with snap-through behavior, the arch structure in publication (Basudhar *et al.* 2008) is researched in this example. Its geometry and force diagram are shown in Fig. 7(a). The curvature radius R of the arch structure is 8m and its central angle θ is 14°. The displacement response at the center A is affected by the parameters thickness t, width w and load F, which are independent of each other. Table 2 describes their corresponding distribution information. Furthermore, the displacement at node A has a snap-through behavior when the arch structure is buckling, i.e. the displacement at node A will abruptly change due to the transition of equilibrium state. Therefore, the whole sample space is divided into two categories: no-buckling (safety) and buckling (failure). Given the symmetry of the arch structure, only a quarter of its finite element model is established. Figs. 7(b) and 7(c) depict the displacements at A under no-buckling and buckling, respectively.

Since the three random parameters obey the different distribution and are non-standard normal random variables, they are firstly converted into standard normal random varibles by Nataf transformation. Subsequently, twelve initial training samples are generated by LHS and their corresponding displacements at center A are obtained by finite element analysis. Similarly, GPC+MPP, GPC+MEMP, ASVC and AGPC-IS respectively run 10 times, and their

Table 2 Distribution information of three variables

Variable	Distribution type	Parameter 1	Parameter 2
w (mm)	Lognormal	400	12
t (mm)	Uniform	7	9
F (N)	Normal	4300	200

Table 3 Average results using different methods for arch structure

Method	N_{call}	$\hat{P}_f$ (10^{-5})	$\delta_{\hat{P}_f}$ (%)	$\varepsilon_{\hat{P}_f}$ (%)
AKDE-IS	9×10^4	8.392	2.03	-
GPC+MPP	>212	6.029	2.11	28.16
GPC+MEMP	125.57	8.161	2.08	2.75
ASVC	>212	9.007	2.12	7.33
AGPC-IS	88.76	8.603	2.07	2.51

*For lognormal distribution, parameters 1 and 2 respectively are the logarithmic mean and logarithmic standard deviation. For uniform distribution, parameters 1 and 2 respectively denote the lower limit and upper limit. For normal distribution, parameters 1 and 2 respectively are the mean and standard deviation.

average results are summarized in Table 3. The "true" failure probability obtained adopting AKDE-IS is about 8.392×10^{-5}, and it takes 9×10^4 finite element simulations and nearly 6 days to complete the reliability analysis. Furthermore, Fig. 8 also compares the variations of $\hat{P}_f$ and ε with N_{it} under different methods. Compared with other

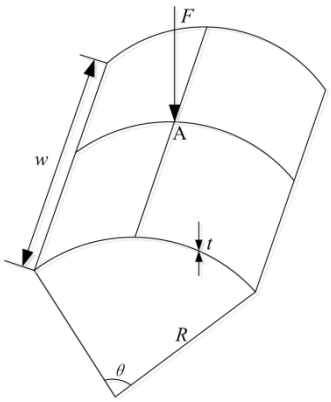

(a) geometry and force diagram

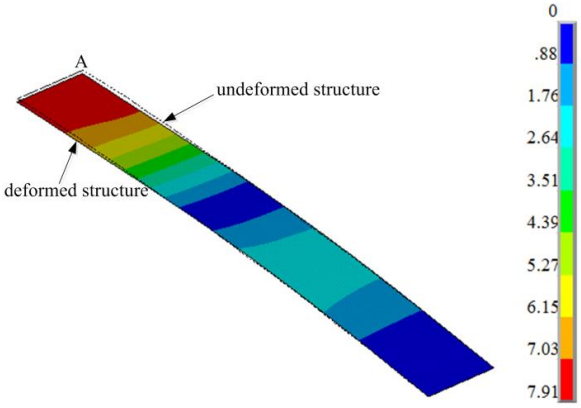

(b) no-buckling

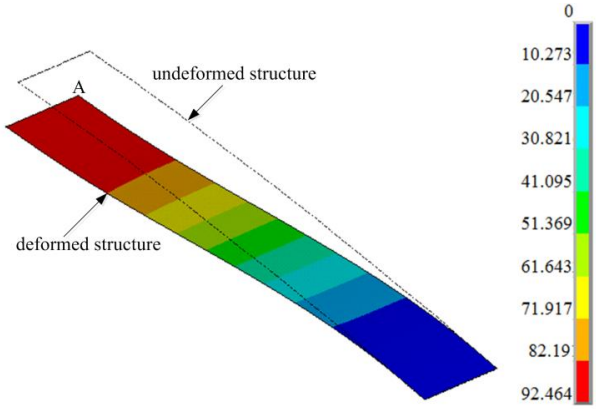

(c) buckling

Fig. 7 Arch structure

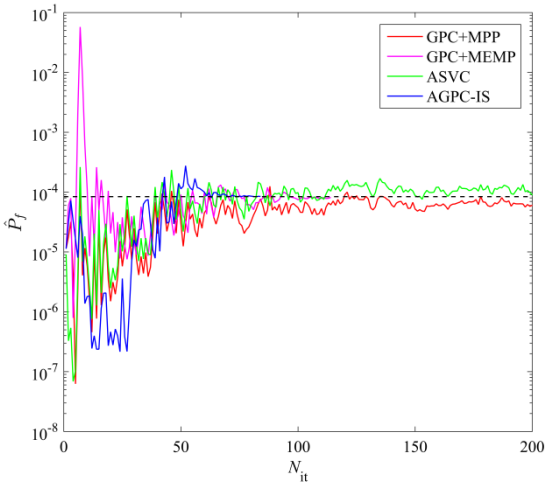

(a) Variations of $\hat{P}_f$ with N_{it}

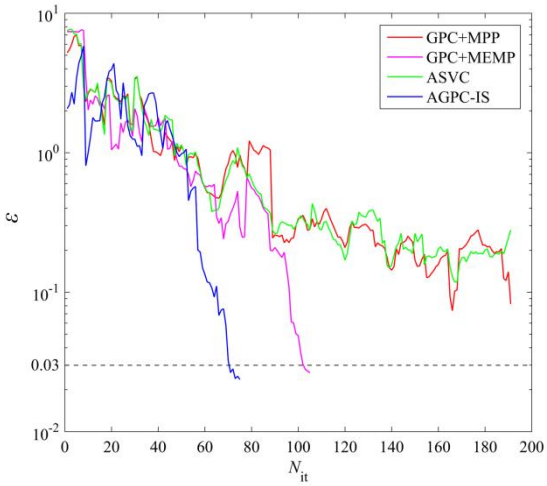

(b) Variations of ε with N_{it}

Fig. 8 Variations of $\hat{P}_f$ and ε with N_{it} by different methods

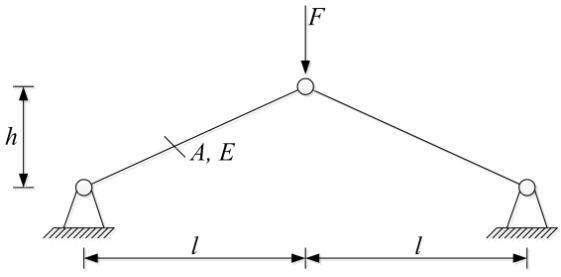

Fig. 9 Two-bars truss structure

methods, AGPC-IS only needs about 88.76 performance function evaluations to obtain satisfactory results, i.e. its efficiency is increased by nearly 29.31%.

4.3 Two-bars truss structure

Truss structures have also received extensive attention due to their discontinuous response. In the publication

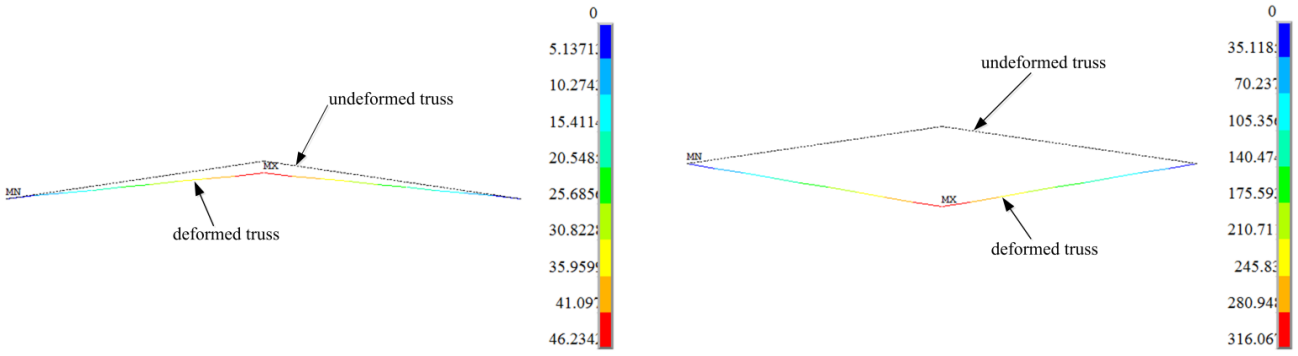

(a) safety state (b) failure state

Fig. 10 Discontinuous displacement of two-bars truss structure

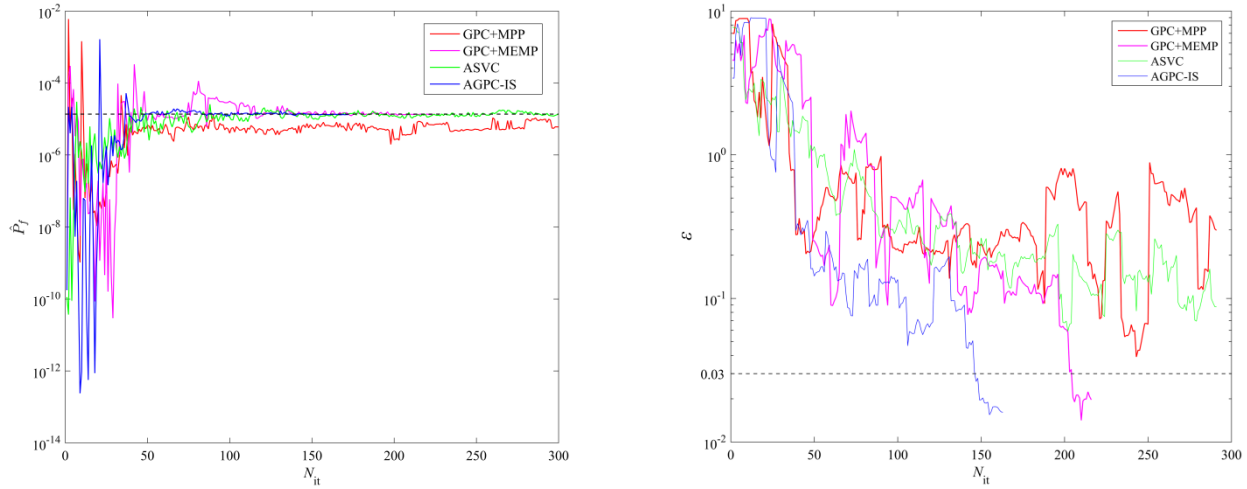

(a) Variations of $\hat{P}_f$ with N_{it} (b) Variations of ε with N_{it}

Fig. 11 Variations of $\hat{P}_f$ and ε with N_{it} using different methods

Table 4 Distribution information of five random variables

Variable	Mean	Standard deviation
l (mm)	1000	10
h (mm)	150	1.5
F (N)	21000	500
E (MPa)	7e4	700
A (mm^2)	275	3

(Niutta *et al.* 2018), the optimization design problem of two-bars truss structure shown in Fig. 9 is researched. In this subsection, it is analyzed from the perspective of structural reliability. The two-bars truss structure contains five independent normal random variables: height h, span $2l$, Young's modulus E, load F and cross-sectional area A. Table 4 lists their corresponding distribution information. The no-buckling displacement (i.e. safety state) and buckling displacement (failure state) at mid-span are depicted in Fig. 10.

Fifteen initial training samples are randomly extracted using LHS. Furthermore, the failure probability obtained by AKDE-IS with 2×10^5 finite element simulations is treated as the 'true' value. The average results of different methods are summarized in Table 5. The variations of $\hat{P}_f$ and ε with N_{it} obtained by different methods are shown in Fig. 11.

Table 5 Average results of two-bars truss structure

Method	N_{call}	$\hat{P}_f$ (10^{-5})	$\delta_{\hat{P}_f}$ (%)	$\varepsilon_{\hat{P}_f}$ (%)
AKDE-IS	2×10^5	1.367	2.39	-
GPC+MPP	>315	0.706	2.42	48.35
GPC+MEMP	229.68	1.328	2.38	2.85
ASVC	>315	1.244	2.45	9.00
AGPC-IS	170.12	1.332	2.41	2.56

Obviously, GPC+MPP and ASVC-IS still do not converge after 315 simulations, while AGPC-IS only needs to perform about 170.12 simulations to converge. In addition, compared with GPC+MEMP, the number of simulations of AGPC-IS is reduced by nearly 60 times.

5. Conclusions

Integrating adaptive Gaussian process classification and importance sampling, this paper proposes a novel reliability analysis method AGPC-IS for structures with discontinuous response and small failure probability.

- An innovative adaptive DoE strategy is developed for gradually improving the accuracy of Gaussian process

classifier. The MCMC algorithm is employed to generate the candidate samples with higher risk of being misclassified, and the Euclidean distance is used to ensure the sampling uniformity. Meanwhile, combining the Kriging surrogate model and the improved distributed hypercube sampling (IHS), the region with high classification uncertainty is identified.

- The quasi-optimal density function of IS is constructed by introducing the MCMC and the adaptive kernel density estimation.
- A more general and accurate stopping criterion is also developed from the perspective of stability of failure probability estimation.
- A piecewise function and two engineering structures are employed to verify the effect of AGPC-IS. Results indicate that compared with other techniques, AGPC-IS needs fewer evaluations of performance function while satisfying the accuracy requirements of reliability analysis. This will significantly improve the efficiency of reliability analysis, especially for the structures with time-consuming finite element analysis.

In general, AGPC-IS can achieve good results when tackling with the structures involving discontinuous response, nonlinear performance function and small failure probability.

Acknowledgments

The financial supports of this research are from the National Natural Science Foundation of China (Grant NO. 51775097 and Grant NO. 51875095). The authors gratefully acknowledge their supports.

References

Alibrandi, U., Alani, A.M. and Ricciardi, G. (2015), "A new sampling strategy for svm-based response surface for structural reliability analysis", *Probabilistic Eng. Mech.*, **41**, 1-12. https://dx.doi.org/10.1016/j.probengmech.2015.04.001

Au, S.K. (2016), "On mcmc algorithm for subset simulation", *Probabilistic Eng. Mech.*, **43**, 117-120. http://dx.doi.org/10.1016/j.probengmech.2015.12.003

Au, S.K. and Beck, J.L. (1999), "A new adaptive importance sampling scheme for reliability calculations", *Structural Safety*, **21**(2), 135-158. https://dx.doi.org/10.1016/S0167-4730(99)00014-4

Au,S.K. and Beck, J.L. (2001), "Estimation of small failure probabilities in high dimensions by subset simulation", *Probabilistic Eng. Mech.*, **16**(4), 263-277. https://dx.doi.org/10.1016/S0266-8920(01)00019-4

Barkhori, M., Shayanfar, M.A., Barkhordari, M.A. and Bakhshpoori, T. (2018), "Kriging-aided cross-entropy-based adaptive importance sampling using gaussian mixture", *J. Sci. Technol. Transactions Civil Eng.*, **43**, 81-88. https://dx.doi.org/10.1007/s40996-018-0143-y

Basudhar, A. and Missoum, S. (2008), "Adaptive explicit decision functions for probabilistic design and optimization using support vector machines", *Comput. Struct.*, **86**(19-20), 1904-1917. https://dx.doi.org/10.1016/j.compstruc.2008.02.008

Basudhar, A., Missoum, S. and Sanchez, A.H. (2008), "Limit state function identification using support vector machines for discontinuous responses and disjoint failure domains", *Probabilistic Eng. Mech.*, **23**(1), 1-11. https://dx.doi.org/10.1016/j.probengmech.2007.08.004

Beachkofski, B.K. and Grandhi, R.V. (2002), "Improved distributed hypercube sampling", *Proceedings of the 43rd AIAA/ASME/ASCE/ASC Structures, Structural Dynamics, and Materials Conference*, Denver, USA, April.

Doh, J., Yang, Q. and Raghavan, N. (2020), "Reliability-based robust design optimization of polymer nanocomposites to enhance percolated electrical conductivity considering correlated input variables using multivariate distributions", *Polymer*, **186**, 122060. http://dx.doi.org/10.1016/j.polymer.2019.122060

Echard, B., Gayton, N. and Lemaire, M. (2011), "Ak-mcs: an active learning reliability method combining kriging and monte carlo simulation", *Struct. Safety*, **33**(2), 145-154. https://dx.doi.org/10.1016/j.strusafe.2011.01.002

Elhewy, A.H., Mesbahi, E. and Pu, Y. (2006), "Reliability analysis of structures using neural network method", *Probabilistic Eng. Mech.*, **21**(1), 44-53. https://dx.doi.org/10.1016/j.probengmech.2005.07.002

En, X.N., Zhang, Y.M. and Huang, X.Z. (2019), "Time-variant reliability analysis of a continuous system with strength deterioration based on subset simulation", *Adv. Manufact.*, **7**(2), 188-198. https://dx.doi.org/10.1007/s40436-019-00252-7

Fang, Y.F. and Teea, K.F. (2017), "Structural reliability analysis using response surface method with improved genetic algorithm", *Struct. Eng. Mech.*, **62**(2), 139-142. https://dx.doi.org/10.12989/sem.2017.62.2.139

Fei, C.W. and Bai, G.C. (2013), "Nonlinear dynamic probabilistic analysis for turbine casing radial deformation using extremum response surface method based on support vector machine", *J. Comput. Nonlinear Dynam.*, **8**(4), 041004. http://dx.doi.org/10.1115/1.4023589

Gao, H.Y., Guo, X.L. and Hu, X.F. (2012), "Crack identification based on kriging surrogate model", *Struct. Eng. Mech.*, **41**(1), 25-41. https://dx.doi.org/10.12989/sem.2012.41.1.025

García-Fernández, Á.F., Tronarp, F. and Särkkä, S. (2019), "Gaussian process classification using posterior linearization", *IEEE Signal Processing Letters*, **26**(5), 735-739. https://dx.doi.org/10.1109/LSP.2019.2906929

Gaspar, B., Teixeira, A.P. and Soares, C.G. (2014), "Assessment of the efficiency of kriging surrogate models for structural reliability analysis", *Probabilistic Eng. Mech.*, **37**, 24-34. https://dx.doi.org/10.1016/j.probengmech.2014.03.011

Guan, X.L. and Melchers, R.E. (2001), "Effect of response surface parameter variation on structural reliability estimates", *Struct. Safety*, **23**(4), 429-444. https://dx.doi.org/10.1016/S0167-4730(02)00013-9

Jagan, J., Samui, P. and Kim, D. (2019), "Reliability analysis of simply supported beam using grnn, elm and gpr", *Struct. Eng. Mech.*, **71**(6), 739-749. https://dx.doi.org/10.12989/sem.2019.71.6.739

Kapoor, A., Grauman, K., Urtasun, R. and Darrell, T. (2009), "Gaussian processes for object categorization", *J. Comput. Vision*, **88**(2), 169-188. https://doi.org/10.1007/s11263-009-0268-3.

Krejsa, M., Janas, P. and Krejsa, V. (2013), "Using doproc method in structural reliability assessment", *Appl. Mech. Mater.*, **300-301**, 860–869. http://dx.doi.org/10.4028/www.scientific.net/AMM.300-301.860

Krejsa, M., Janas, P. and Krejsa, V. (2016), "Application of the doproc method in solving reliability problems", *Appl. Mech. Mater.*, **821**, 717–724. http://doi.org/10.4028/www.scientific.net/AMM.821.717

Li, X., Gong, C., Gu, L., Gao, W., Jing, Z. and Su, H. (2018), "A sequential surrogate method for reliability analysis based on radial basis function", *Struct. Safety*, **73**, 42-53. https://dx.doi.org/10.1016/j.strusafe.2018.02.005

Napa-García, G.F., Beck, A.T. and Celestino, T.B. (2017), "Reliability analyses of underground openings with the point

estimate method", *Tunnelling Underground Space Technol.*, **64**, 154-163. http://dx.doi.org/10.1016/j.tust.2016.12.010

Nguyen, T.N.A., Abdesselam, B. and Phung, S.L. (2019), "A scalable hierarchical gaussian process classifier", *IEEE Transactions on Signal Processing*, **67**(11), 3042-3057. https://dx.doi.org/10.1109/TSP.2019.2911251

Niutta, C.B., Wehrle, E.J., Duddeck, F. and Belingardi, G. (2018), "Surrogate modeling in design optimization of structures with discontinuous responses", *Struct. Multidisciplinary Opt.*, **57**(5), 1857-1869. https://dx.doi.org/10.1007/s00158-018-1958-7

Pan, Q.J. and Dias, D. (2017), "An efficient reliability method combining adaptive support vector machine and monte carlo simulation", *Structural Safety*, **67**, 85-95. https://dx.doi.org/10.1016/j.strusafe.2017.04.006

Peng, L.F., Su, G.S. and Zhao, W. (2014), "Fast analysis of structural reliability using gaussian process classification based dynamic response surface method", *Appl. Mech. Mater.*, **501-504**, 1067-1070. https://dx.doi.org/10.4028/www.scientific.net/AMM.501-504.1067

Qin, S., Hu, J., Zhou, Y.L., Zhang, Y. and Kang, J. (2019), "Feasibility study of improved particle swarm optimization in kriging metamodel based structural model updating", *Struct. Eng. Mech.*, **70**(5), 513-524. https://dx.doi.org/10.12989/sem.2019.70.5.513

Rodrigues, F., Pereira, F.C. and Ribeiro, B. (2014), "Gaussian process classification and active learning with multiple annotators", *Proceedings of the 31st International Conference on Machine Learning*, Beijing, China, June.

Roudak, M.A. and Karamloo, M. (2019). "Establishment of non-negative constraint method as a robust and efficient first-order reliability method", *Appl. Math. Modell.*, **68**, 281-305. http://dx.doi.org/10.1016/j.apm.2018.11.021

Shayanfar, M.A., Barkhordari, M.A., Barkhori, M. and Rakhshanimehr, M. (2017), "An adaptive line sampling method for reliability analysis", *J. Sci. Technol. Transactions Civil Eng.*, **41**(3), 275-282. https://dx.doi.org/10.1007/s40996-017-0070-3

Su, G., Jiang, J., Yu, B. and Xiao, Y. (2015), "A gaussian process-based response surface method for structural reliability analysis", *Struct. Eng. Mech.*, **56**(4), 549-567. https://dx.doi.org/10.12989/sem.2015.56.4.549

Sun, S., Zhong, P., Xiao, H. and Wang, R. (2015), "Active learning with gaussian process classifier for hyperspectral image classification", *IEEE Transactions on Geoscience and Remote Sensing*, **53**(4), 1746-1760. https://dx.doi.org/10.1109/TGRS.2014.2347343

Sun, S., Zhong, P., Xiao, H. and Wang, R. (2017), "Lif: a new kriging based learning function and its application to structural reliability analysis", *Reliability Eng. Syst. Safety*, **157**, 152-165. https://dx.doi.org/10.1016/j.ress.2016.09.003

Vahedi, J. Ghasemi, M.R. and Miri, M. (2018), "Structural reliability assessment using an enhanced adaptive kriging method", *Struct. Eng. Mech.*, **66**(6), 677-691. https://dx.doi.org/10.12989/sem.2018.66.6.677

Wang, F. and LI, H. (2017), "Stochastic response surface method for reliability problems involving correlated multivariates with non-gaussian dependence structure: analysis under incomplete probability information", *Comput. Geotechnics*, **89**, 22-32. http://dx.doi.org/10.1016/j.compgeo.2017.02.008

Wang, J. and Sun, Z.L. (2018), "The stepwise accuracy-improvement strategy based on the kriging model for structural reliability analysis", *Struct. Multidisciplinary Opt.*, **58**(2), 595-612. https://dx.doi.org/10.1007/s00158-018-1911-9

Jian, W., Zhili, S., Qiang, Y. and Rui, L. (2017), "Two accuracy measures of the kriging model for structural reliability analysis", *Reliability Eng. Syst. Safety*, **167**, 494-505. https://dx.doi.org/10.1016/j.ress.2017.06.028

Winerstein, S.R. (1988), "Nonlinear vibration models for extremes and fatigue", *J. Eng. Mech.*, **114**(10), 1772-1790. http://dx.doi.org/10.1061/(ASCE)0733-9399(1988)114:10(1772)

Xiong, F., Xiong, Y., Greene, S., Chen, W. and Yang, S. (2010), "A new sparse grid based method for uncertainty propagation", *Struct. Multidisciplinary Opt.*, **41**(3), 335–349. http://dx.doi.org/10.1007/s00158-009-0441-x

Xu, J. and Wang, D. (2019), "Structural reliability analysis based on polynomial chaos, voronoi cells and dimension reduction technique", *Reliability Eng. Syst. Safety*, **185**, 329-340. https://dx.doi.org/10.1016/j.ress.2019.01.001

Yang, X., Liu, Y., Mi, C. and Wang, X. (2018), "Active learning kriging model combining with kernel-density-estimation-based importance sampling method for the estimation of low failure probability", *J. Mech. Design*, **140**(5), 051402. https://dx.doi.org/10.1115/1.4039339

Yao, W., Tang, G., Wang, N. and Chen, X. (2019), "An improved reliability analysis approach based on combined form and beta-spherical importance sampling in critical region", *Struct. Multidisciplinary Opt.*, **60**(1), 35-58. https://dx.doi.org/10.1007/s00158-019-02193-y.

Yonezawa, M., Okuda, S. and Kobayashi, H. (2009), "Structural reliability estimation based on quasi ideal importance sampling simulation", *Struct. Eng. Mech.*, **32**(1), 55-69. https://dx.doi.org/10.12989/sem.2009.32.1.055

Yuan, X., Lu, Z., Zhou, C. and Yue, Z. (2013), "A novel adaptive importance sampling algorithm based on markov chain and low-discrepancy sequence", *Aerosp. Sci. Technol.*, **29**(1), 253-261. https://dx.doi.org/10.1016/j.ast.2013.03.008

Yun, W.Y., Lu, Z.Z. and Jiang, X. (2017), "A modified importance sampling method for structural reliability and its global reliability sensitivity analysis", *Struct. Multidisciplinary Opt.*, **57**(4), 1625-1641. https://dx.doi.org/10.1007/s00158-017-1832-z.

Yun, W.Y., Lu, Z.Z. and Jiang, X. (2018), "An efficient reliability analysis method combining adaptive kriging and modified importance sampling for small failure probability", *Struct. Multidisciplinary Opt.*, **58**(4), 1383-1393. https://dx.doi.org/10.1007/s00158-018-1975-6

Zhang, J.H., Xiao, M. and Gao, L. (2018), "An active learning reliability method combining kriging constructed with exploration and exploitation of failure region and subset simulation", *Reliability Eng. Syst. Safety*, **188**, 90-102. https://dx.doi.org/10.1016/j.ress.2019.03.002

Zhang, Y., Sun, Z., Yan, Y., Yu, Z. and Wang, J. (2019), "An efficient adaptive reliability analysis method based on kriging and weighted average misclassification rate improvement", *IEEE Access*, **7**(1), 94954-94965. https://dx.doi.org/10.1109/ACCESS.2019.2928332.

Zhao, H.B., Li, S.J. and Ru, Z.L. (2017), "Adaptive reliability analysis based on a support vector machine and its application to rock engineering", *Appl. Math. Modell.*, **44**, 508-522. https://dx.doi.org/10.1016/j.apm.2017.02.020

Zhao, W.T., Shi, X.Y. and Tang, K. (2016), "A response surface method based on sub-region of interest for structural reliability analysis", *Struct. Eng. Mech.*, **57**(4), 587-602. https://dx.doi.org/10.12989/sem.2016.57.4.587

PL